

High-field ordered and superconducting phases in the heavy-fermion compound $\text{PrOs}_4\text{Sb}_{12}$

P.-C. Ho, N. A. Frederick, V. S. Zapf, E. D. Bauer, T. D. Do, and M. B. Maple

Department of Physics and Institute for Pure and Applied Physical Sciences, University of California, San Diego, La Jolla, California 92093-0360, USA

A. D. Christianson and A. H. Lacerda

National High Magnetic Field Laboratory/LANL, Los Alamos, New Mexico 87545, USA

(Received 17 February 2003; published 29 May 2003)

The filled-skutterudite compound $\text{PrOs}_4\text{Sb}_{12}$, the first example of a Pr-based heavy-fermion superconductor, displays superconductivity with $T_c \sim 1.85$ K and has an effective mass $m^* \sim 50m_e$, where m_e is the free-electron mass. For magnetic fields above 4.5 T, sharp features in the normal-state electrical resistivity, magnetization, specific-heat, and thermal-expansion data suggest the occurrence of a phase transition at high fields. This high-field ordered phase in the normal state may be associated with a combination of crystalline electric fields, Zeeman splitting, and quadrupolar ordering. We present an investigation of the electrical resistivity and magnetization of $\text{PrOs}_4\text{Sb}_{12}$ as a function of temperature between 350 mK and 3.5 K and magnetic field up to 18 T. The data reveal a detailed phase boundary of the high-field ordered phase as well as the lower critical field H_{c1} and the onset field of the peak effect in the superconducting state of $\text{PrOs}_4\text{Sb}_{12}$.

DOI: 10.1103/PhysRevB.67.180508

PACS number(s): 74.70.Tx, 65.40.-b, 71.27.+a, 75.30.Mb

I. INTRODUCTION

The filled-skutterudite compound $\text{PrOs}_4\text{Sb}_{12}$ displays superconductivity with $T_c \approx 1.85$ K and has an effective mass $m^* \sim 50m_e$.¹ This compound is the first example of a Pr-based heavy-fermion superconductor; all other known heavy-fermion superconductors are intermetallic compounds of the rare-earth element Ce or the actinide element U. Inelastic neutron-scattering experiments, along with an analysis of magnetic-susceptibility $\chi(T)$ and specific-heat $C(T)$ data^{2,3} for a cubic crystalline electric field (CEF), are consistent with a Pr^{3+} energy scheme consisting of a nonmagnetic Γ_3 doublet ground state (0 K), a Γ_5 triplet first excited state (~ 8 K), and higher energy Γ_4 triplet (~ 133 K) and Γ_1 singlet (~ 320 K) excited states. The heavy-fermion properties of the Pr-based compounds PrInAg_2 and $\text{PrFe}_4\text{P}_{12}$ have been attributed to the interaction of the charges of the conduction electrons with the electric quadrupole moments of the $\text{Pr}^{3+}\Gamma_3$ nonmagnetic doublet ground state in the CEF.^{4,5} The evidence for a $\text{Pr}^{3+}\Gamma_3$ ground state in $\text{PrOs}_4\text{Sb}_{12}$ indicates that the electric quadrupolar fluctuations may be responsible for the heavy-fermion state in this compound and could also be involved in the superconductivity.¹⁻³

For magnetic fields H above ~ 4.5 T, sharp features in measurements of the normal-state electrical resistivity^{2,6} $\rho(T)$, magnetization^{3,7} $M(H)$, specific heat⁸ $C(T)$, thermal expansion⁹ $\alpha(T)$, and magnetostriction¹⁰ $\lambda(T)$ of $\text{PrOs}_4\text{Sb}_{12}$ indicate that a phase transition is induced at high fields. The origin of the high-field ordered phase (HFOP) is still under investigation but may be related to the crossing of the Zeeman levels of the Γ_3 and Γ_5 CEF states and a corresponding change of the ground state at high fields.⁸ In this paper, we present further results of our investigation of $\text{PrOs}_4\text{Sb}_{12}$, utilizing electrical-resistivity measurements up to 18 T and magnetization measurements with magnetic field H \parallel $[111]$ and $[001]$ crystallographic directions up to 5.5 T.

II. EXPERIMENTAL DETAILS

The $\text{PrOs}_4\text{Sb}_{12}$ samples studied were single crystals grown in Sb flux.¹¹ X-ray-diffraction measurements confirmed the cubic $\text{LaFe}_4\text{P}_{12}$ -type structure.¹² The $\rho(H, T)$ measurements were made with a Linear Research LR 700 4-wire ac bridge operating at 16 Hz with constant current amplitudes of $100 \mu\text{A}$ ($0 \text{ T} \leq H \leq 10 \text{ T}$) and $300 \mu\text{A}$ ($10 \text{ T} \leq H \leq 18 \text{ T}$), and in a transverse geometry in a ^3He - ^4He dilution refrigerator⁶ ($0 \text{ T} \leq H \leq 10 \text{ T}$) and a ^3He cryostat ($10 \text{ T} \leq H \leq 18 \text{ T}$). The $M(H, T)$ measurements were performed in a ^3He Faraday magnetometer with a gradient field of 1 kOe/cm in fields up to 5.5 T and at temperatures between 0.4 K and 2 K.

III. RESULTS AND DISCUSSION

A. Normal-state properties

The behavior of the electrical resistivity ρ below 4.2 K and 18 T is summarized in Fig. 1. Figures 1(a) [Ref. 6] and 1(b) show $\rho(T)$ data in various constant fields, while Fig. 1(c) displays isotherms of $\rho(H)$. In this temperature range, the phonon contribution to ρ is negligible.¹³ The $\rho(T, H)$ data in Figs. 1(b) and 1(c) were taken on a different $\text{PrOs}_4\text{Sb}_{12}$ sample and in a different cryostat. The absolute value of the resistivity is sample dependent in the present work, probably due to irregular sample shapes and the presence of microcracks in the samples. Thus, the $\rho(T, H)$ data in Figs. 1(b) and 1(c) were normalized to those in Fig. 1(a) by comparing the $\rho(T)$ data at 10 T for both samples, which differ by a factor of ~ 0.44 . The sharp drops in $\rho(T)$ below 2.5 T are due to the superconducting transition. A kink in the $\rho(T)$ curves develops above ~ 4.5 T and becomes most pronounced between 7 T and 11 T, and then gradually subsides as H increases further. This kink is apparently related to the

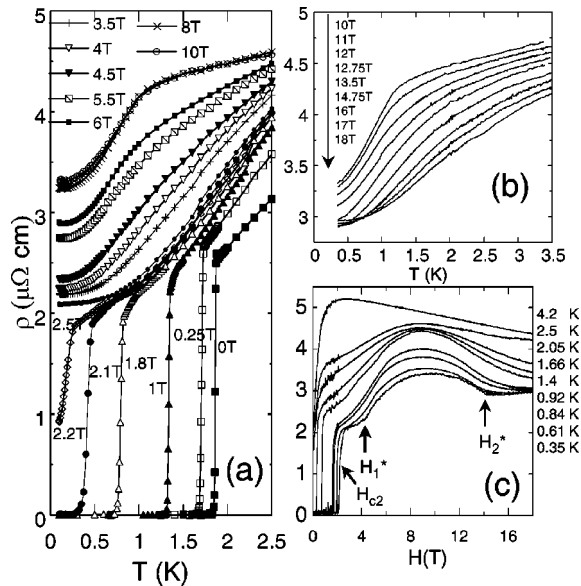


FIG. 1. (a) (Ref. 6) and (b) Electrical resistivity ρ vs T in various magnetic fields H up to 18 T for $\text{PrOs}_4\text{Sb}_{12}$ single crystals. (c) ρ vs H at various temperatures T up to 4.2 K. The rapid drop in ρ to zero for $H < 2.5$ T is due to the superconducting transition, while the shoulder in $\rho(T)$ at ~ 1 K above 4.5 T and sharp kinks in $\rho(H)$ (marked as H_1^* and H_2^*) below 0.7 K are due to a HFOP (Ref. 8).

occurrence of a HFOP which will be discussed later (Fig. 4). The $\rho(T)$ data between 8 T and 10 T almost overlap with each other [Fig. 1(a) and Ref. 6]. The $\rho(H)$ data below 1 K reach a maximum at ~ 9 T as shown in Fig. 1(c), while the dome-shaped feature becomes more pronounced as T decreases. Two sharp kinks (H_1^* and H_2^*) become easily identified below 0.61 K and mark the boundary of the HFOP.⁶⁻⁸

The ρ vs H isotherms reveal that ρ is enhanced in the HFOP over a linear interpolation of ρ from outside this region [Fig. 1(c)]. Due to the crystalline electric field and the Zeeman splitting of $\text{Pr}^{3+} J=4$ states, the 4- f electron populations in each level will change with temperature. These changes will affect the interactions between 4- f and conduction electrons that, in turn, will affect the transport properties.¹⁴⁻¹⁷ Calculations of $\rho(H, T)$ for such a case, in which an exchange interaction¹⁴⁻¹⁶ and an aspherical Coulomb interaction^{14,16,17} between the Zeeman split 4- f and conduction electrons have been added to the cubic CEF Hamiltonian with a Γ_3 ground state at $H=0$ T, agree qualitatively with the experimental ρ vs H isotherms (detailed calculations are described in Ref. 18). The calculated ρ vs H isotherms are plotted in Fig. 2 and can be compared with the experimental ρ vs H isotherms in Fig. 1(c). In this calculation, we found that a Γ_1 ground state will not produce the same features as we observe in the measurements of the $\rho(H)$ isotherms.¹⁸ This provides further support for a Γ_3 ground state in $\text{PrOs}_4\text{Sb}_{12}$.

The magnetization $M(H)$ measurements were performed with the applied magnetic field oriented along the $[111]$ and $[001]$ crystallographic directions of a single crystal of $\text{PrOs}_4\text{Sb}_{12}$ for $0 \leq H \leq 5.5$ T. Only the isothermal $M(H)$ data for $H \parallel [111]$ are shown in Fig. 3. A kink (at H_1^*) ap-

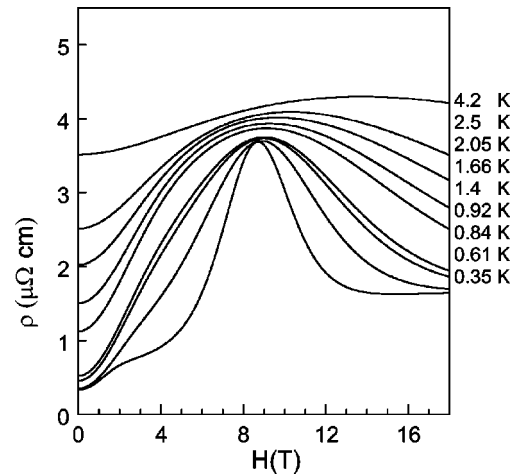


FIG. 2. Calculated ρ vs H isotherms based on a CEF Hamiltonian including equal amounts of the magnetic exchange and aspherical Coulomb interactions assuming a Γ_3 ground state (Ref. 18). The dome-shaped structure is qualitatively comparable to Fig. 1(c).

pears in $M(H)$ curves above 4.5 T and cannot be resolved above 0.8 K for $H \leq 5.5$ T. This feature is apparently associated with the onset of the HFOP. We found that the fields where the $M(H)$ kinks occur are the same for $H \parallel [111]$ and $[001]$ (i.e., no anisotropy). In contrast, Tenya *et al.* reported small but noticeable anisotropy in the location of the boundary of the HFOP.⁷

In previous work, a HFOP was identified from the kinks in magnetoresistivity $\rho(H, T)$ data,^{2,6} kinks in magnetization $M(H, T)$ data,^{3,7} peaks in specific heat $C(T, H)$ data,⁸ and peaks in thermal-expansion $\alpha(T, H)$ data.⁹ From our new set of $\rho(H, T)$ measurements, shown in Figs. 1(b) and 1(c), the

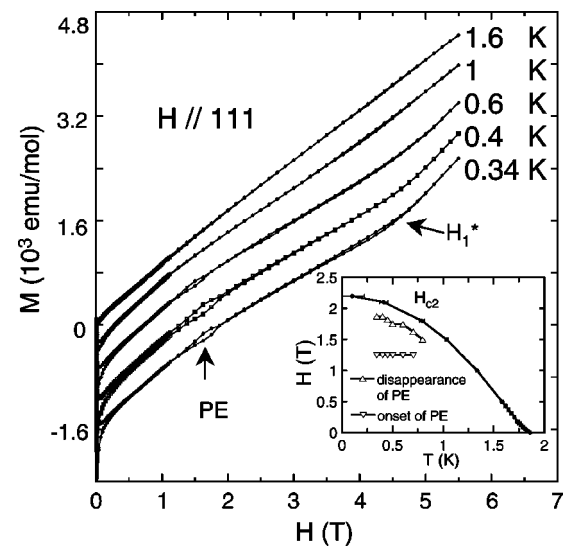


FIG. 3. M vs H ($\parallel [111]$) at various temperatures. The $M(H)$ kink occurs at H_1^* , the boundary of the high-field ordered phase. Inset: Fields at which the PE appears and disappears, deduced from $M(H)$ data of a $\text{PrOs}_4\text{Sb}_{12}$ single crystal with $H \parallel [111]$. H_{c2} is derived from the superconducting transition observed in the $\rho(T)$ data (Refs. 1 and 6).

upper boundary of the HFOP can be determined. The H - T phase diagram, depicting the superconducting and the HFOP regions, is constructed in Fig. 4. Recent magnetostriction and additional thermal-expansion measurements by Oeschler *et al.* also indicate a similar phase boundary for the HFOP.¹⁰ Since an increase in the magnetic field would induce mixing of the ground state and the low-lying first excited state, the HFOP may be driven by the crossing of the upper level of the Γ_3 doublet and the lowest level of the Γ_5 triplet states at ~ 4.5 T and another crossing between the lowest levels of the Γ_3 and Γ_5 states at ~ 10 T, which changes the ground state.⁸ In Fig. 4, the dashed line below 4.5 T and 2 K that connects the peaks in $d\rho/dT$ (Ref. 6) and intersects the HFOP is a measure of the Zeeman splitting between the Pr^{3+} ground state and the first excited state. The nearly temperature-independent boundary of the HFOP at ~ 14.5 T resembles the antiferroquadrupolar ordered phase observed in PrPb_3 ,¹⁹ which also has a Γ_3 ground state. It is plausible that the HFOP in $\text{PrOs}_4\text{Sb}_{12}$ has the same origin. However, the antiferroquadrupolar ordered phase observed in PrPb_3 exhibits strong anisotropy above 1 T. We did not observe such an anisotropy in the HFOP from the magnetization data of $\text{PrOs}_4\text{Sb}_{12}$ along [001] and [111] between 4.5 and 5.5 T, although the anisotropy at these fields may not be large enough to resolve. Neutron-scattering experiments²⁰ on our powdered single crystals of $\text{PrOs}_4\text{Sb}_{12}$ did not detect any signs of a HFOP.

B. Superconducting-state properties

A peak effect (PE) in the superconducting state that had an onset at ~ 1.25 T and disappeared at ~ 0.3 T below the

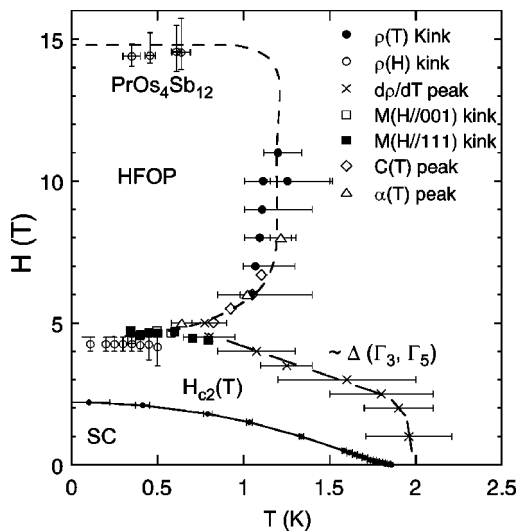


FIG. 4. H - T phase diagram for $\text{PrOs}_4\text{Sb}_{12}$. The superconducting-state (SC) phase boundary is derived from the electrical-resistivity $\rho(T, H)$ data (Refs. 1 and 6). The HFOP is deduced from the features observed in $\rho(T, H)$, $C(T, H)$ (Ref. 8) $M(H, T)$ ($H \parallel [001]$ and $[111]$), and $\alpha(T, H)$ (Ref. 9). The dashed line drawn through the points where $d\rho/dT$ exhibits a peak above 1 K is a measure of the energy difference between the Pr^{3+} Γ_3 ground and Γ_5 first excited state (Refs. 8 and 3).

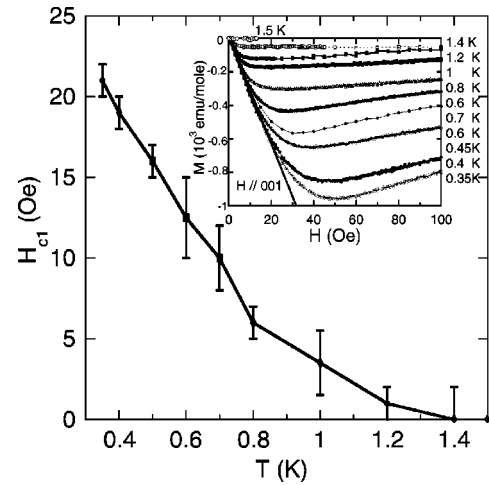


FIG. 5. Lower critical field H_{c1} vs T . Inset: M vs H ($\parallel [001]$) below 100 Oe at various temperatures. H_{c1} is defined as the field where the curve departs from the initial linear region.

upper critical field $H_{c2}(T)$ was also observed in $M(H)$ measurements (Fig. 3). The fields at which the PE appears and disappears are plotted in the inset of Fig. 3. According to recent thermal conductivity measurements on a $\text{PrOs}_4\text{Sb}_{12}$ single crystal in a magnetic field,²¹ there are two distinct superconducting phases in the H - T plane with twofold and fourfold rotation symmetries in the basal plane. The phase boundary between the twofold and fourfold symmetry superconducting phases is at $H \approx 0.75$ T for $T \approx 0.5$ K. The onset field of our PE occurs at a higher field and for the fields below the PE region, no anomaly is observed in our $M(H)$ curves. It is not clear whether the PE is related to the twofold and fourfold symmetry superconducting phases²¹ or to pinning from crystal defects or impurities. However, recent transverse-field muon spin rotation measurements²² with $H = 200$ Oe indicated that $\text{PrOs}_4\text{Sb}_{12}$ has a nearly isotropic superconducting energy gap in the superconducting state.

Figure 5 shows the lower critical field H_{c1} vs T determined for $H \parallel [001]$. $H_{c1}(0)$ is quite small, ~ 23 Oe. The magnetic susceptibility χ in the Meissner state was found to be $-31.5 \text{ cm}^3/\text{mol}$ (or $-1/[0.613(4\pi)]$). The demagnetization factor of the sample is estimated to be ~ 0.45 ,^{23,24} resulting in a superconducting volume fraction of $\sim 74\%$. The Ginzburg-Landau parameter is estimated to be $\kappa \approx (H_{c2}/H_{c1})^{1/2} \sim 31$ with $H_{c2} \sim 2.19$ T and $H_{c1} \sim 23$ Oe. This value is a factor of 10 larger than that estimated from the relation $\kappa = \lambda/\xi_0 \sim 3$, where the penetration depth $\lambda \sim 344 \text{ \AA}$ was taken from muon spin resonance measurements²² and the coherence length $\xi_0 \sim 113 \text{ \AA}$ was estimated from the initial slope of H_{c2} .⁶ The discrepancy may arise from error in the estimates of H_{c1} due to the residual field in the superconducting magnet or to different qualities of samples used in the various measurements.

IV. SUMMARY

In summary, we have reported electrical-resistivity and magnetization measurements on $\text{PrOs}_4\text{Sb}_{12}$ at high magnetic fields and determined the H - T phase diagram below 18 T.

Aspherical Coulomb and magnetic exchange scattering between $4f$ and conduction electrons can qualitatively describe the dome-shaped features observed in the $\rho(H)$ data and provide evidence that Γ_3 is the ground state at zero magnetic field.

The high-field ordered-phase boundary is determined from kinks in $\rho(H,T)$ and $M(H,T)$ data. The HFOP is confined to a region on the H - T plane between ~ 4.5 T and 14.5 T, and below ~ 1 K. Measurements of $M(H,T)$ for $H < 5.5$ T, parallel to the [001] and [111] directions, did not exhibit appreciable anisotropy. In analogy with the behavior of PrPb_3 , the HFOP may be associated with antiferroquadrupolar order.

The $M(H,T)$ measurements revealed a small value for the lower critical field $H_{c1}(0)$ of ~ 23 Oe, and a value for the upper critical field $H_{c2}(0)$ of ~ 2.19 T, yielding a Ginzburg-Landau parameter $\kappa \sim 31$. A peak effect was observed which

had an onset at ~ 1.3 T between 0.35 K and 0.7 K and disappeared at a field that tracked the $H_{c2}(T)$ curve which had an offset of ~ 0.3 T. No evidence in the $M(H,T)$ data was found for a crossover between two superconducting phases with different order-parameter symmetry as reported by Izawa *et al.*²¹

ACKNOWLEDGMENTS

This research was supported by the U.S. Department of Energy under Grant No. DEFG-03-86ER-45230, the U.S. National Science Foundation under Grant No. DMR-00-72125, and the NEDO international Joint Research Program, and the work at the NHMFL Pulsed Field Facility (Los Alamos National Laboratory) was performed under the auspices of the NSF, the State of Florida and the U.S. Department of Energy.

-
- ¹E.D. Bauer, N.A. Frederick, P.-C. Ho, V.S. Zapf, and M.B. Maple, Phys. Rev. B **65**, 100506 (2002).
- ²M.B. Maple, P.-C. Ho, V.S. Zapf, N.A. Frederick, E.D. Bauer, W.M. Yuhasz, F.M. Woodward, and J.W. Lynn, J. Phys. Soc. Jpn. **71**, Suppl., 23 (2002).
- ³M.B. Maple, P.-C. Ho, N.A. Frederick, V.S. Zapf, W.M. Yuhasz, and E.D. Bauer, Acta Phys. Pol. B **34**, 919 (2003).
- ⁴A. Yatskar, W.P. Beyermann, R. Movshovich, and P.C. Canfield, Phys. Rev. Lett. **77**, 3637 (1996).
- ⁵H. Sato, Y. Abe, H. Okada, T.D. Matsuda, K. Abe, H. Sugawara, and Y. Aoki, Phys. Rev. B **62**, 15 125 (2000).
- ⁶P.-C. Ho, V.S. Zapf, E.D. Bauer, N.A. Frederick, and M.B. Maple, Int. J. Mod. Phys. B **16**, 3008 (2002).
- ⁷K. Tenya, N. Oeschler, P. Gegenwart, F. Steglich, N.A. Frederick, E.D. Bauer, and M.B. Maple, Acta Phys. Pol. B **34**, 995 (2003).
- ⁸R. Vollmer, A. Faißt, C. Pfleiderer, H.v. Lohneysen, E.D. Bauer, P.-C. Ho, V.S. Zapf, and M.B. Maple, Phys. Rev. Lett. **90**, 057001 (2003).
- ⁹N. Oeschler, P. Gegenwart, F. Steglich, N.A. Frederick, E.D. Bauer, and M.B. Maple, Acta Phys. Pol. B **34**, 919 (2003).
- ¹⁰N. Oeschler, F. Weickert, P. Gegenwart, P. Thalmeier, F. Steglich, E. D. Bauer, and M. B. Maple (unpublished).
- ¹¹E.D. Bauer, A. Ślebarski, E.J. Freeman, C. Sirvent, and M.B. Maple, J. Phys.: Condens. Matter **13**, 4495 (2001).
- ¹²W. Jeitshco and D. Braun, Acta Crystallogr., Sect. B: Struct. Crystallogr. Cryst. Chem. **33**, 3401 (1977).
- ¹³The T dependence of the normal-state resistivity of $\text{LaOs}_4\text{Sb}_{12}$ is negligible for $0.1 \text{ K} \leq T \leq 2.5 \text{ K}$ and $0 \text{ T} \leq H \leq 8 \text{ T}$ (unpublished).
- ¹⁴P. Fulde and I. Peschel, Adv. Phys. **21**, 1 (1972).
- ¹⁵N.H. Anderson, P.E. Gregers-Hansen, E. Holm, and H. Smith, Phys. Rev. Lett. **32**, 1321 (1974).
- ¹⁶Z. Fisk and D.C. Johnson, Solid State Commun. **22**, 359 (1977).
- ¹⁷R.J. Elliott, Phys. Rev. **94**, 564 (1954).
- ¹⁸N.A. Frederick and M.B. Maple, cond-mat/0303471, J. Phys. Condens. Matt. (to be published).
- ¹⁹T. Tayama, T. Sakakibara, K. Kitami, M. Yokoyama, K. Tenya, H. Amitsuka, D. Aoki, Y. Ōnuki, and Z. Kletowski, J. Phys. Soc. Jpn. **70**, 248 (2001).
- ²⁰J. W. Lynn and M. B. Maple (unpublished).
- ²¹K. Izawa, Y. Nakajima, J. Goryo, Y. Matsuda, S. Osaki, H. Sugawara, H. Sato, P. Thalmeier, and K. Maki, Phys. Rev. Lett. **90**, 117001 (2003).
- ²²D.E. MacLaughlin, J.E. Sonier, R.H. Heffner, O.O. Bernal, B.-L. Young, M.S. Rose, G.D. Morris, E.D. Bauer, T.D. Do, and M.B. Maple, Phys. Rev. Lett. **89**, 157001 (2002).
- ²³D.N. Cronmeyer, J. Appl. Phys. **70**, 2911 (1991).
- ²⁴The $\text{PrOs}_4\text{Sb}_{12}$ single crystal used in the magnetization measurements had an irregular bar shape with $a \times b \times c \approx 2.2 \text{ mm} \times 0.72 \text{ mm} \times 0.61 \text{ mm}$ and $H \parallel c$. It was assumed to be equivalent to an ellipsoid with $c/a \sim b/a \sim 0.3$